

Device- and System-Level Thermal Packaging for Electric-Drive Technologies

Yogendra Joshi, Samuel Graham, Satish Kumar
Georgia Institute of Technology
June 25, 2021

Project ID# elt251

*DOE Vehicle Technologies Office
2021 Annual Merit Review*

Timeline

- Project start date: April 2019
- Project end date: March 2024
- Percent: 40%

Budget

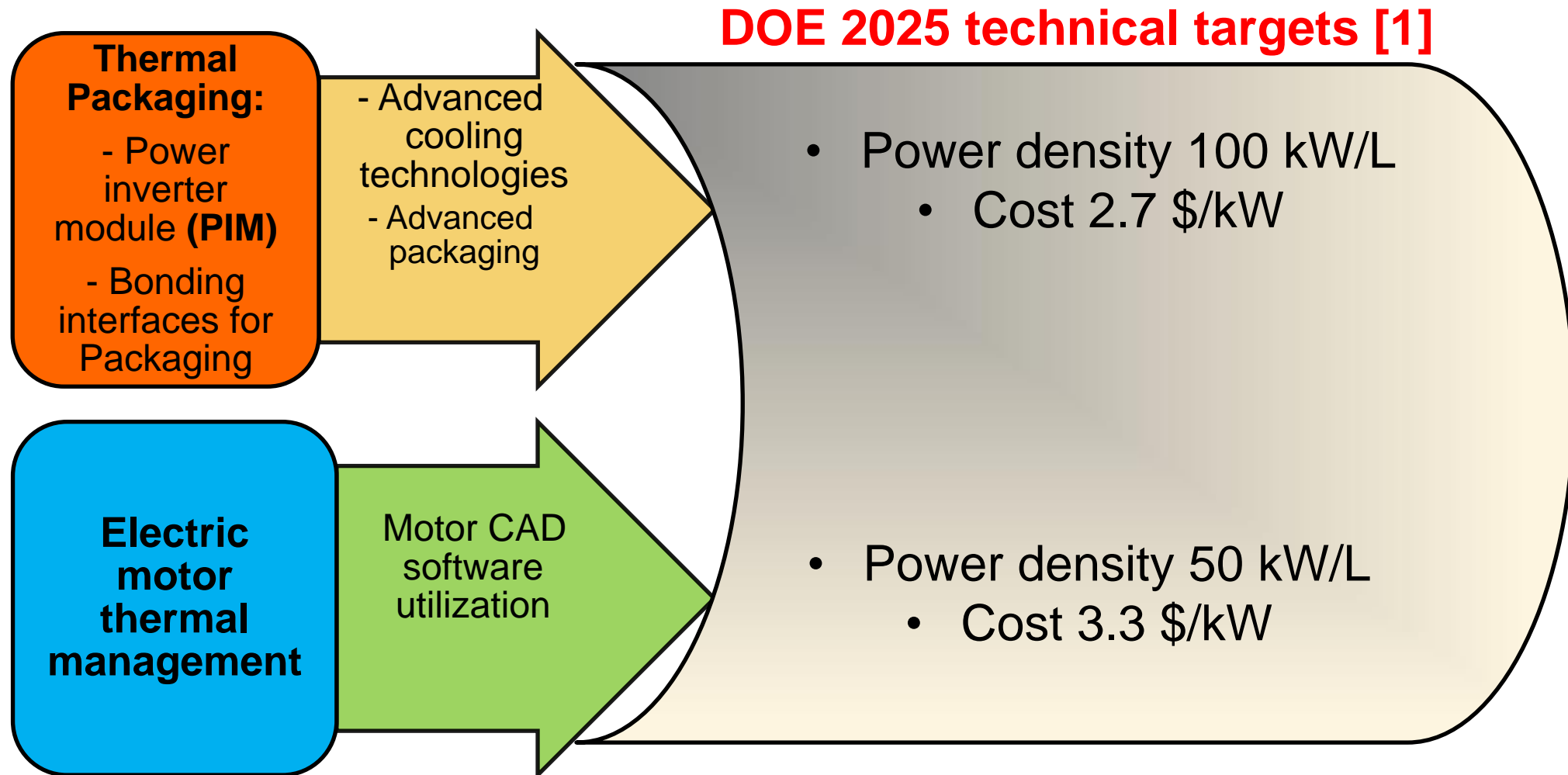
- Total project funding: \$1.5M
 - DOE share: \$1.5M
 - Contractor share: \$0
- Funding for FY 2020: \$300K
- Funding for FY 2021: \$300K

Barriers

- Cost, power density and reliability challenges in vehicle electrification using Wide Band Gap (WBG) semiconductor devices
- Thermal management techniques required to achieve targeted power densities in power inverter module and electric motors
- New packaging concept to enable transition to WBG semiconductor devices.

Partners

- National Renewable Energy Laboratory (NREL)
- Oak Ridge National Laboratory (ORNL)



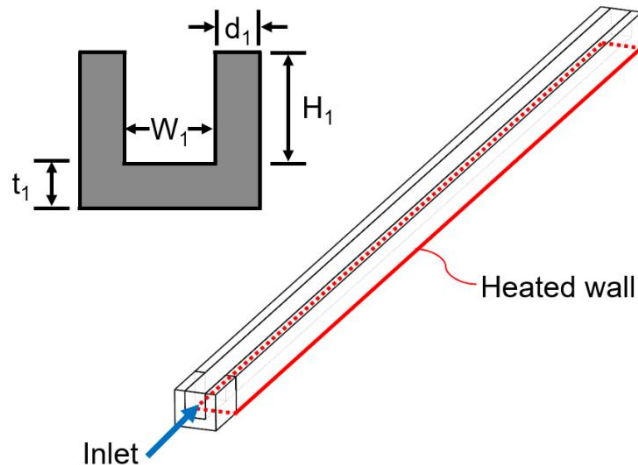
[1] U.S. DRIVE Electrical and Electronics Technical Team Roadmap, 2017

MICROCHANNEL SIMULATION: TWO-PHASE FLOW AND HEAT TRANSFER MODELLING FOR COLD PLATE

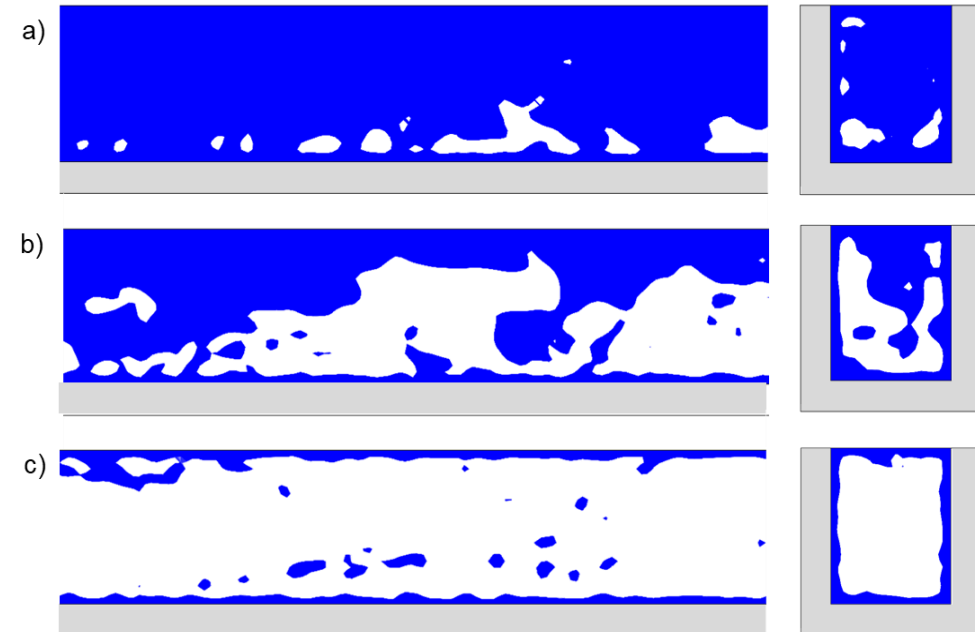
- Objective:
 - Numerically investigate passive methods of mitigating microchannel thermohydraulic instabilities
 - Compare to a baseline case without instability mitigation.



- Framework
 - Three microchannels to be compared to baseline
 - Volume-of-fluid method with mass transfer



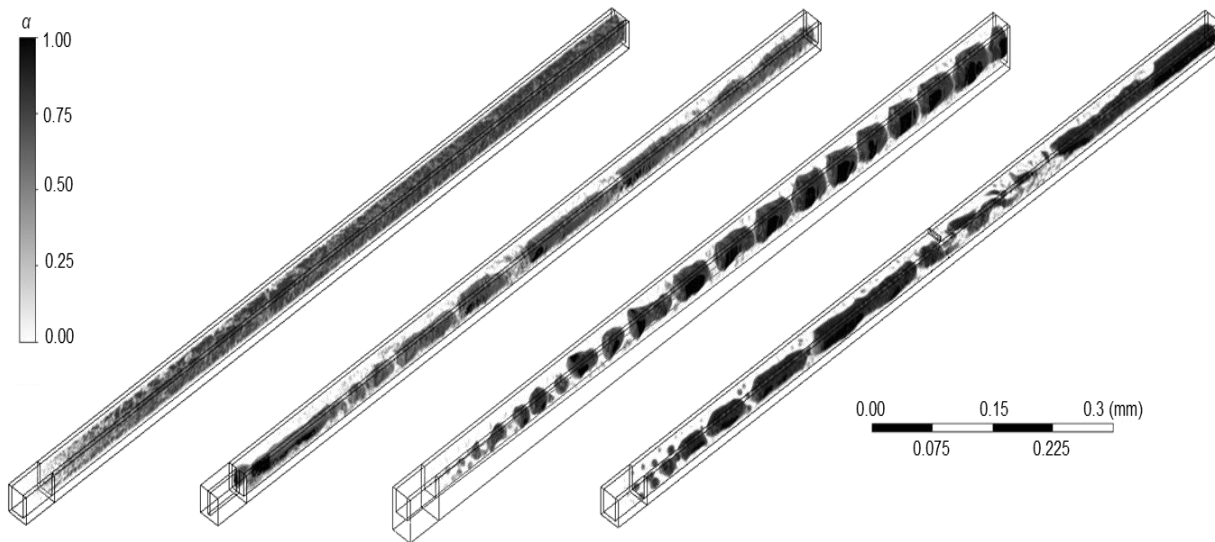
Computational geometry for baseline straight microchannel



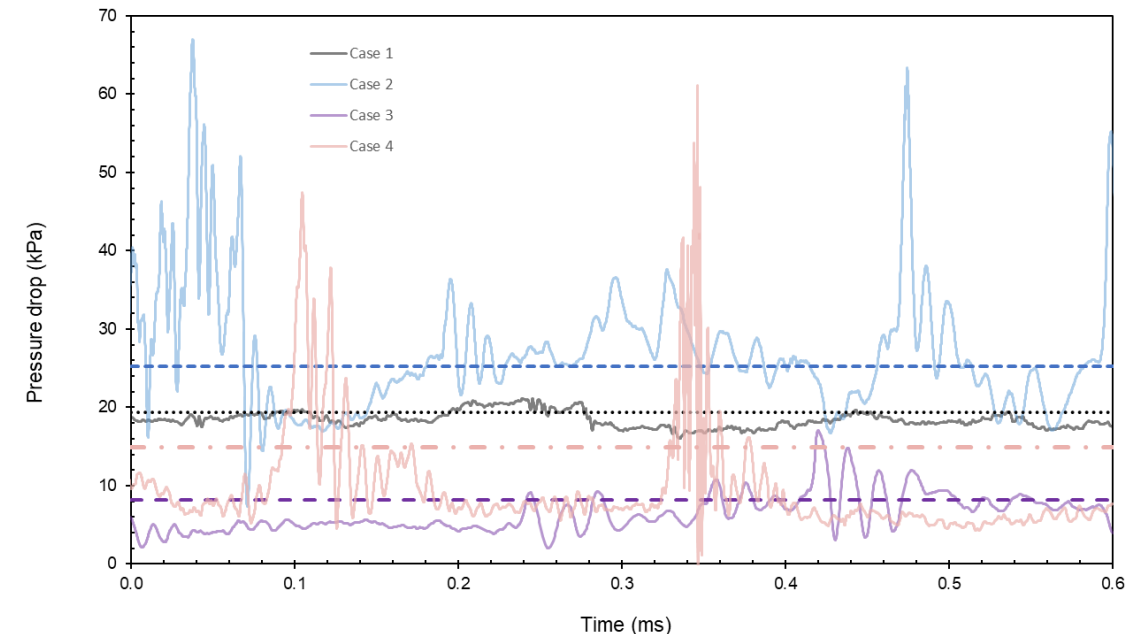
Liquid and vapor regime visualization in baseline case showing magnified side and frontal views of a) bubbly flow, b) churn flow, and c) confined annular flow phase contours

MICROCHANNEL SIMULATION: CFD MODELLING FOR COLD PLATE

- Performed simulation on four different geometries
 - For case 4, instead of having 1 inlet with a flow bypass, we elected to have two inlets (as jetting effect was negligible without inlet restriction)
 - Harirchian and Garimella [1] predicted 1) churn/confined annular 2) churn/confined annular 3) slug 4) slug then annular after the jet
- Thermohydraulic performance quantified, trends consistent w/ literature
 - Heat transfer coefficient sees significant increase for cases 3 and 4, negligible increase for case 2.
 - Pressure drop improves significantly for cases 3 and 4, due to decreased acceleration pressure drop from bigger area and collapsed bubbles, respectively.



Void fractions volume renderings for each case after quasi-steady-state, showing flow regimes in good agreement with first flow regime map

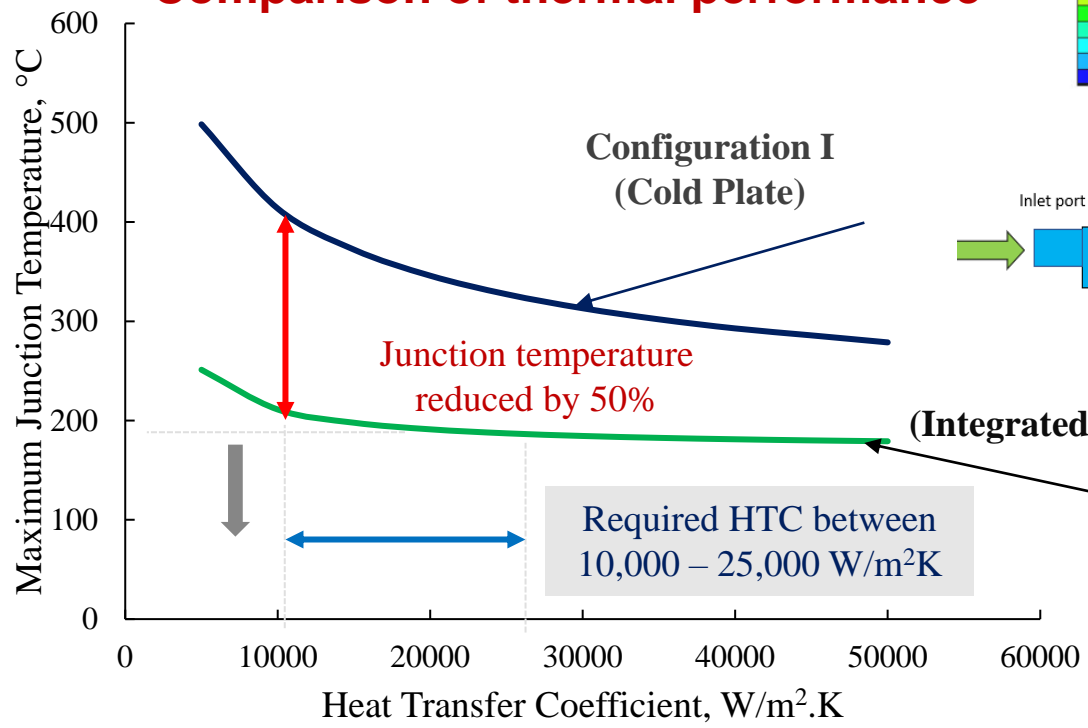


Transient and average pressure drop over 0.6 ms of quasi-steady state operation (~5,000 time steps)

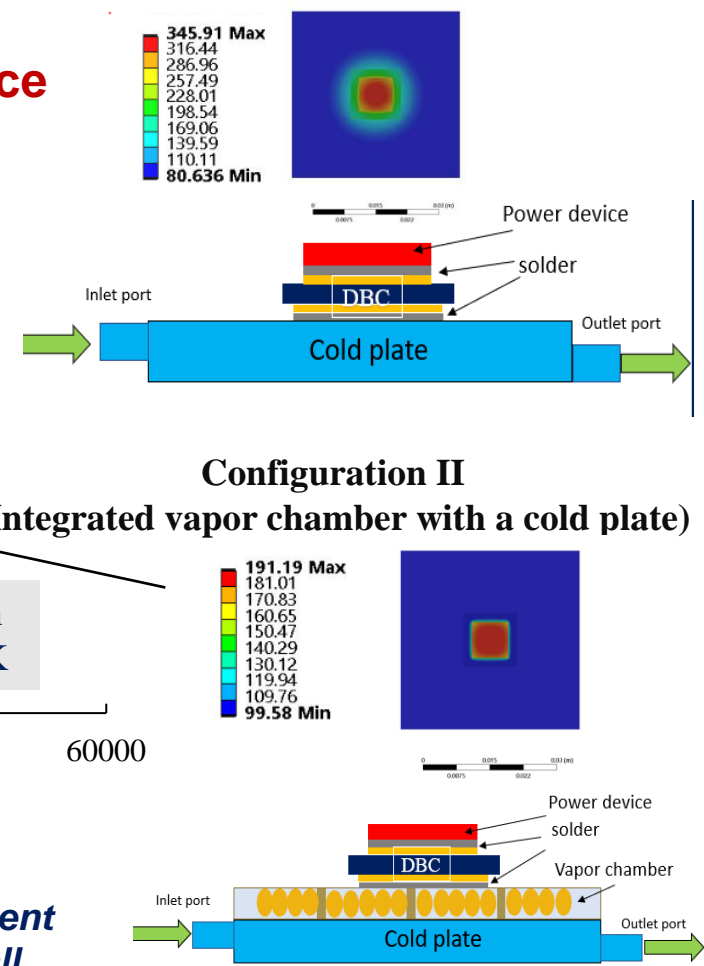
VAPOR CHAMBER (VC) DEVELOPMENT: COMPUTATIONS

- Performed thermal analysis on unit cell geometry for 640 W at coolant inlet temperature 80°C, and compared the results with and without VC
- Junction temperature is reduced by 50% for heat transfer coefficient (HTC) between 10,000 – 25,000 W/m²K on cold plate
- Result shows VC provides more heat spreading and a uniform heat temperature distribution across the stack

Comparison of thermal performance



Thermal performance of proposed stack arrangement (integrated VC with a cold plate setup) and overall temperature maps



THIN VC FOR POWER ELECTRONICS PACKAGING



1. Copper sheet

2. Laminate top surface with negative photoresist

3. Place a Teflon piece and expose to UV light

4. Remove the photoresist film in photoresist developer

5. Perform etching in copper etching differential

6. Final product

1. Etch copper sheet

2. Uniformly distribute copper particles on inverted mold

3. Assemble part 1 and 2 in a test rig

4. Sinter at 750 °C for 3 hours in a forming gas environment at 15 liters/min in furnace

Final vapor chamber

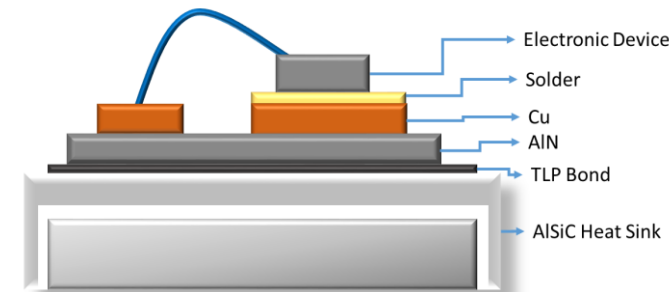
Total thickness is 0.5 mm

40 mm

TECHNICAL ACCOMPLISHMENTS – THERMAL PACKAGING

LOW THERMAL RESISTANCE BONDED THERMAL INTERFACES

- Novel Package design employs **transient liquid phase bonding (TLP)** in attaching dielectric AlN substrate directly to AlSiC heat sink
 - Lower process temperature
 - Minimized CTE mismatch – up to 84% drop
 - Enhanced fatigue and thermal performance
 - Increase in power density, specific power and cost reduction

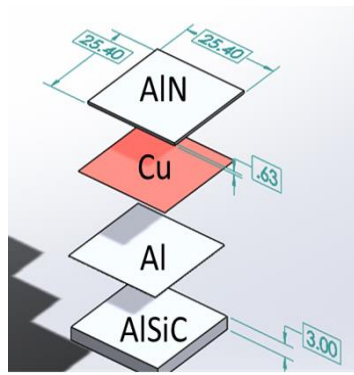


Transient liquid phase bonding (TLP) Process

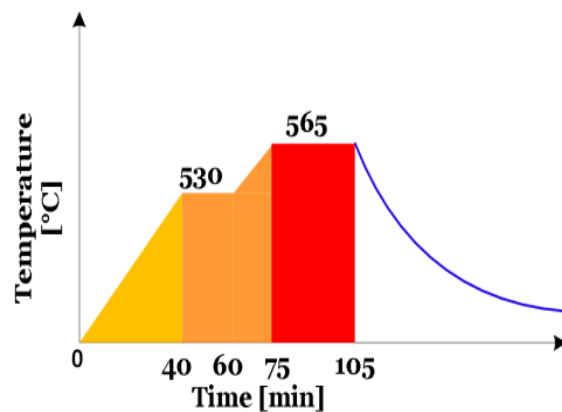
- ✓ Assembly: AlN, Cu and Al foils, and AlSiC layers combined in a graphite rig
- ✓ Heating: Assembly heated in furnace following temperature profile
- ✓ Cooling: Bonding temperature down to 565°C from 1070°C (DBC)



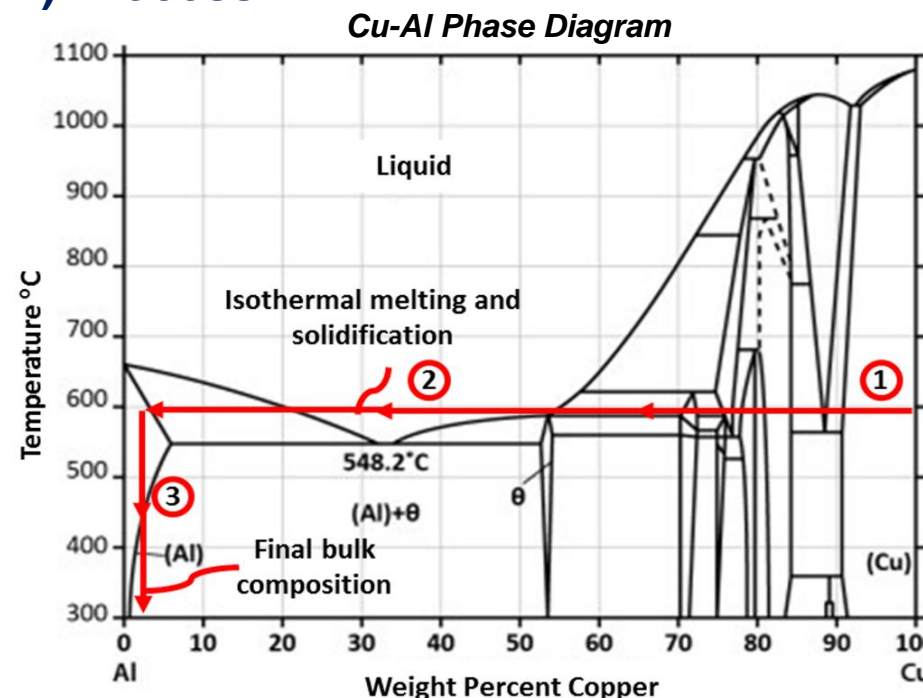
Bonding Rig



Bond Stack

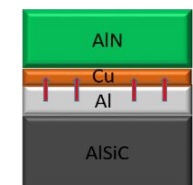


Temperature Profile



Cu-Al Phase Diagram

1. Cu - Al Diffusion



2. Transient Liquid Phase



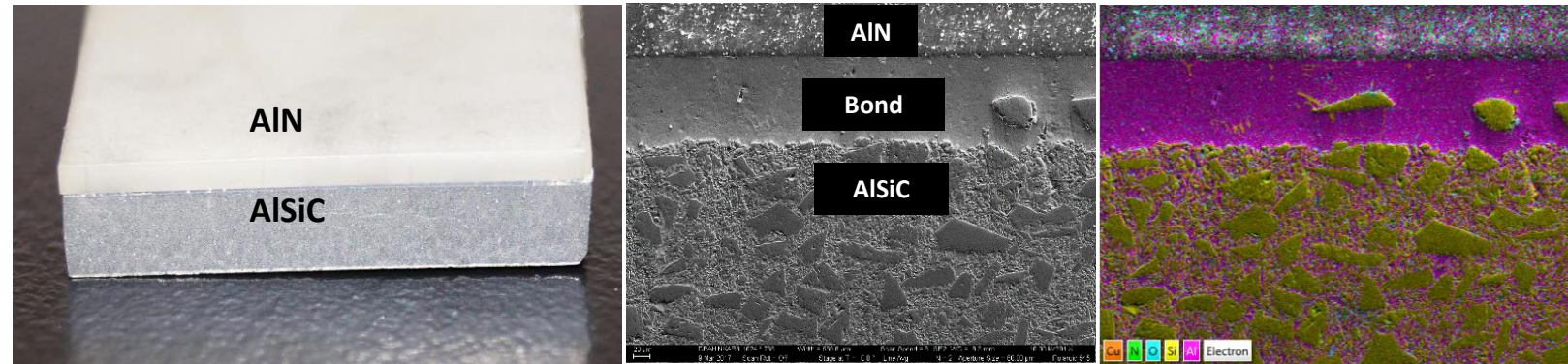
3. Solidification at high temperature



LOW THERMAL RESISTANCE BONDED INTERFACES: RESULT

Bonded Sample:

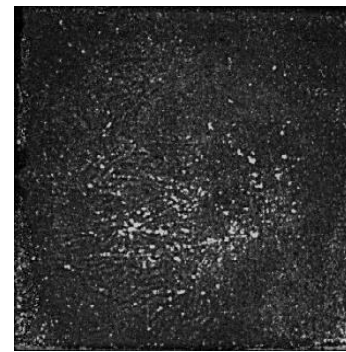
- SiC particles migrate into the bond
- 130 ± 12 W/m-K thermal conductivity of TLP bond
 - Thermal resistance reduced by at least 2.28 times compared to best solders available



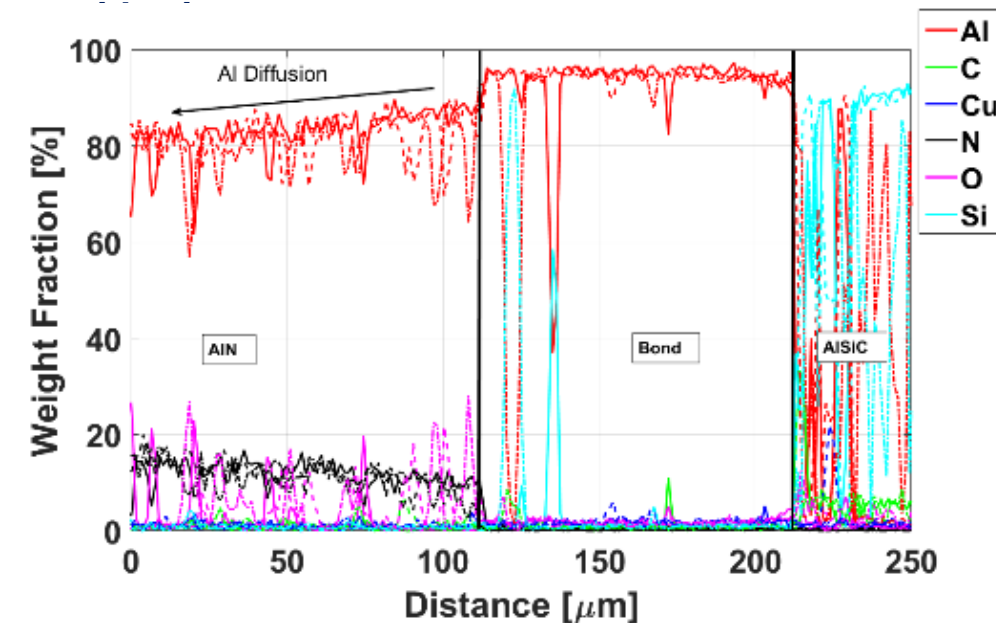
AIN – AISiC coupons bonded using Cu-Al alloy and

Bond Properties: C-Sam results:

- C-Sam images shows a homogeneous bond for void fraction as low as 2%. Fatigue tests show no failures after 1200 cycles at -40 °C to 150 °C(5°C/min). 1400 hours of aging at 150°C show no change in void fraction. DBC fails between 100-200 cycles.

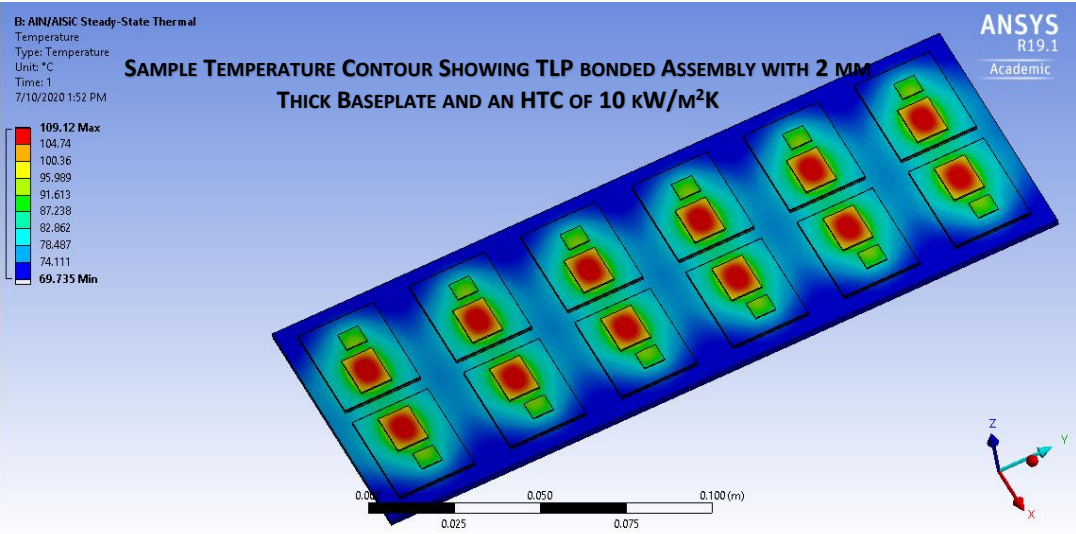


C-SAM of bond line void fraction

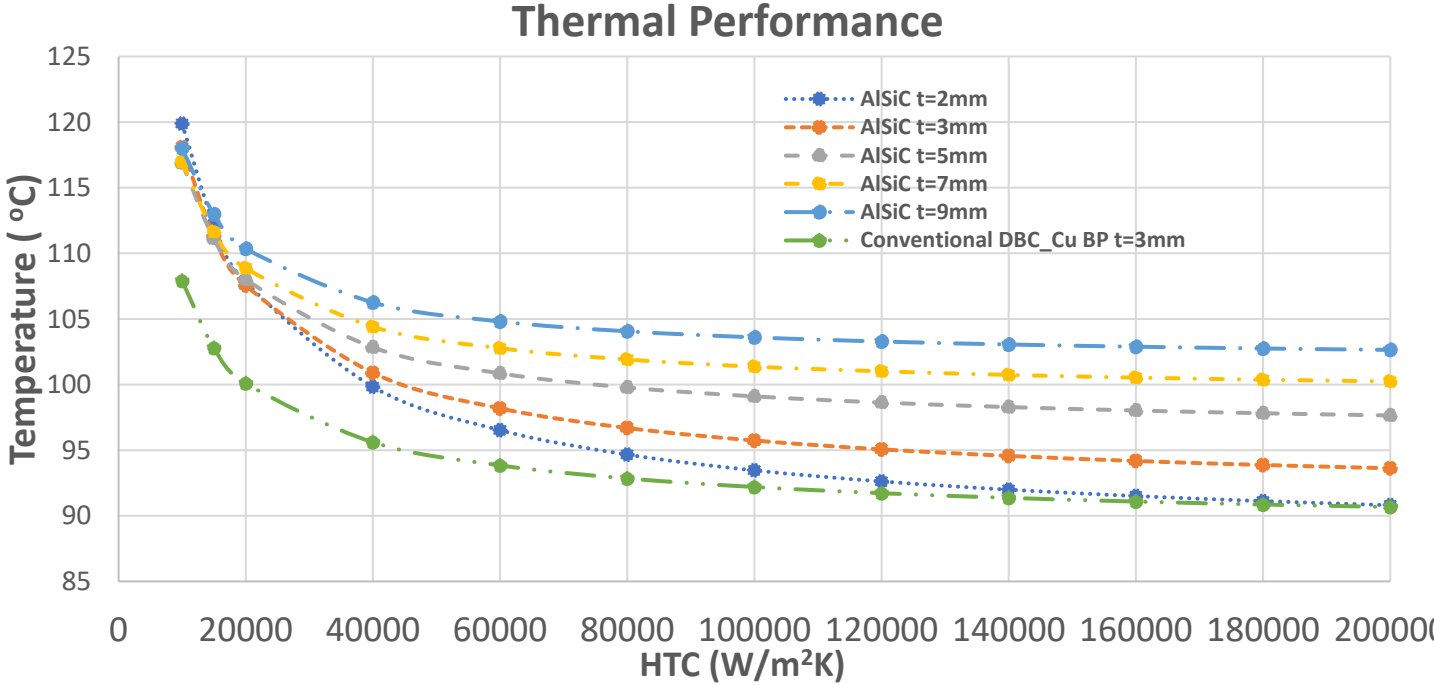


LOW THERMAL RESISTANCE BONDED THERMAL INTERFACES: NUMERICAL MODELING

- Performed thermal analysis on TLP bonded AlSiC with varying thickness compared to DBC assembly
- At low HTC values, Cu baseplate aids in spreading heat efficiently due to higher convective resistance.
- For HTC values $\geq 40 \text{ kW/m}^2\text{K}$, thinner AlSiC baseplates perform comparatively well with $\text{max } \Delta T < 5^\circ\text{C}$ between 2mm thick AlSiC and DBC_Cu



Temperature map showing TLP bonded assembly with 2mm thick baseplate and an HTC of $10 \text{ kW/m}^2\text{K}$



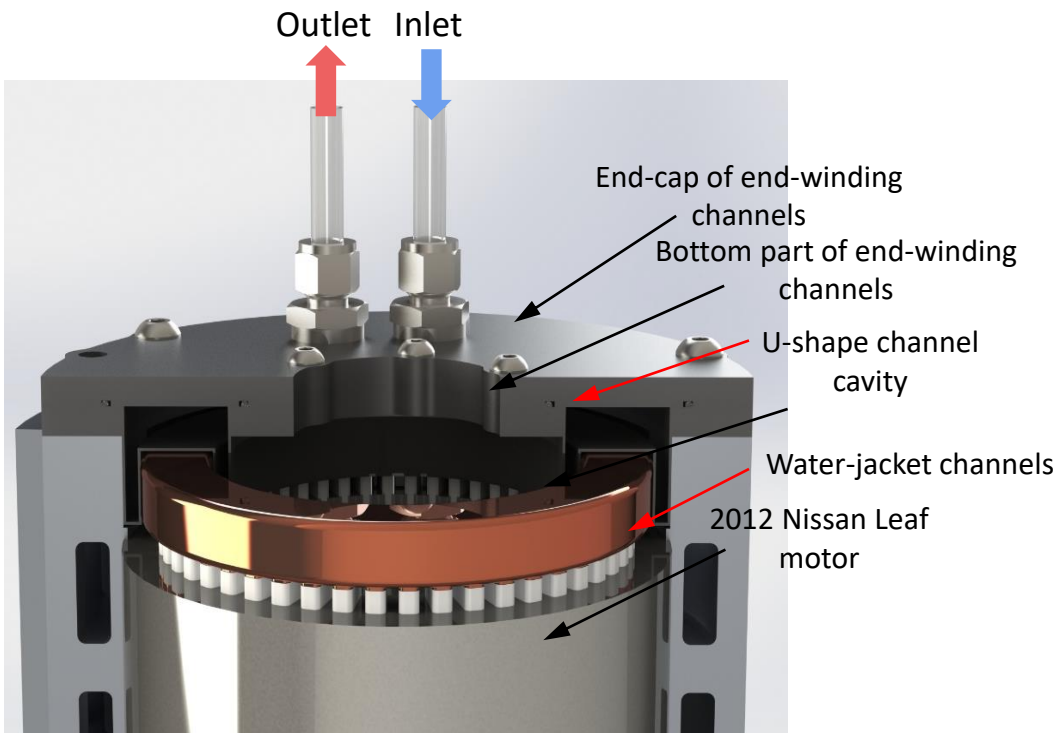
Effect of HTC on junction temperature for various AlSiC thicknesses

TECHNICAL ACCOMPLISHMENTS – ELECTRIC MOTOR THERMAL MANAGEMENT

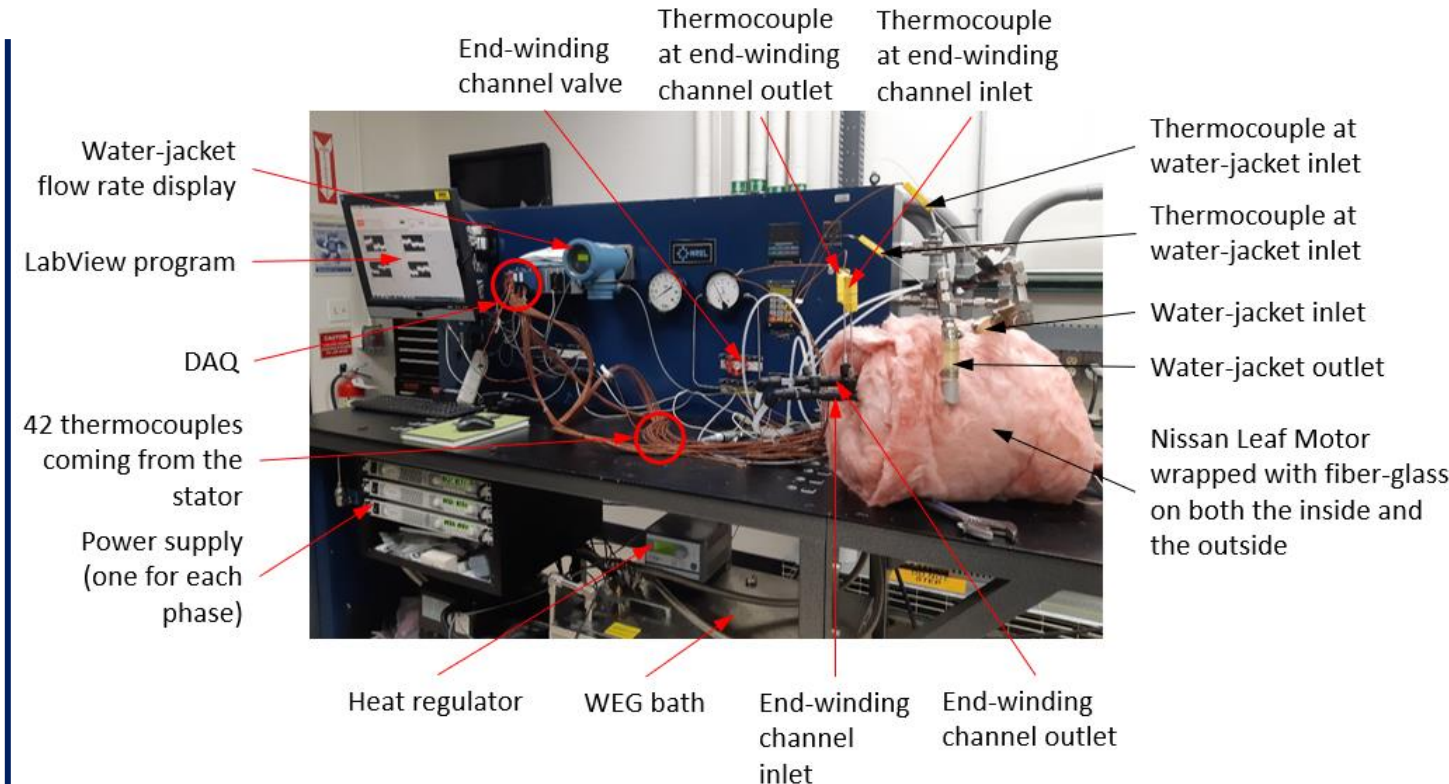
PROPOSED END-WINDING SOLUTION AND EXPERIMENTAL SETUP

Objectives:

- Compare the thermal performance of the motor when using water-jacket alone and when using water-jacket with end-winding channel.
- Derive the equivalent heat transfer coefficient (HTC) of end-winding channel.



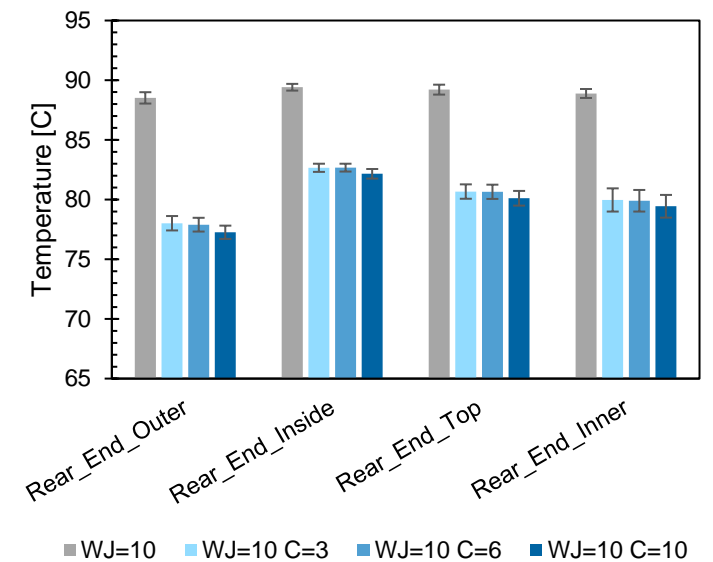
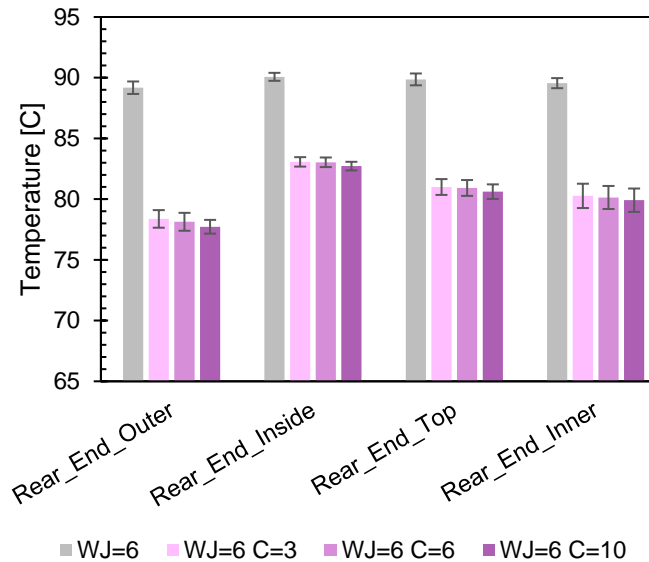
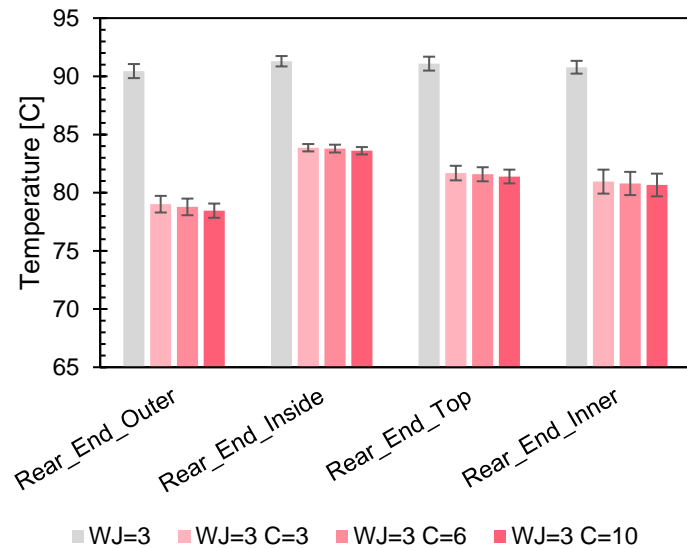
Cross-section view of end-winding channels



Experimental setup (Tests performed at NREL)

Design and testing of a new end-winding cooling system (end-winding channel): RESULTS

- One plot represents a fixed flow rate for the water-jacket.
- Legend description (example with left plot):
 - “WJ=3” means flow rate in the water-jacket = 3 L/min and no end-winding channel has been used.
 - “WJ=3 C=3” means flow rate in the water-jacket = 3 L/min and flow rate in end-winding channel = 3 L/min.
 - “WJ=3 C=6” means flow rate in the water-jacket = 3 L/min and flow rate in end-winding channel = 6 L/min.
 - “WJ=3 C=10” means flow rate in the water-jacket = 3 L/min and flow rate in end-winding channel = 10 L/min.



Average temperatures on each side of rear end-windings (outer side, inner side, top side and inside) at different flow rates in both the water-jacket and the end-winding channel

TAKE-AWAYS

- When the end-winding channel is used in addition to the water-jacket, we have a significant temperature drop on each side of the end-winding.
- We have a good cooling performance even with low flow rates in the channels.

MILESTONES

Milestone	Type	Description	Status
Multiphysics modeling framework demonstration	Technical	Approach for performing multi-physics modeling of SiC and GaN packaging demonstrated	Completed
Vapor chamber for SiC and GaN power packaging demonstrated	Technical	Demonstrate vapor chamber performance at 1 kW/cm ² at device operation below 200 °C	Completed
Compact modeling-based co-design and optimization framework demonstration	Technical	Case study to demonstrate application of the developed framework	Completed
Cold plate for high- temperature electronics demonstrated	Technical	Establish single-phase cold plate design with integrated vapor chamber for operation at 1 kW/cm ² and below 200 °C device temperature	Completed
Demonstration of power electronics thermal packaging technologies for high heat fluxes and temperatures	Go/No Go	Establish viable thermal packaging approaches for power device operation temperatures below 200 °C and 1 kW/cm ² . Alignment with above performance measures will be demonstrated.	In Progress

Note – Due to COVID-19, three months of campus labs closure in 2020 has caused delays in the last milestone.

FY2021:

➤ Thermal Packaging:

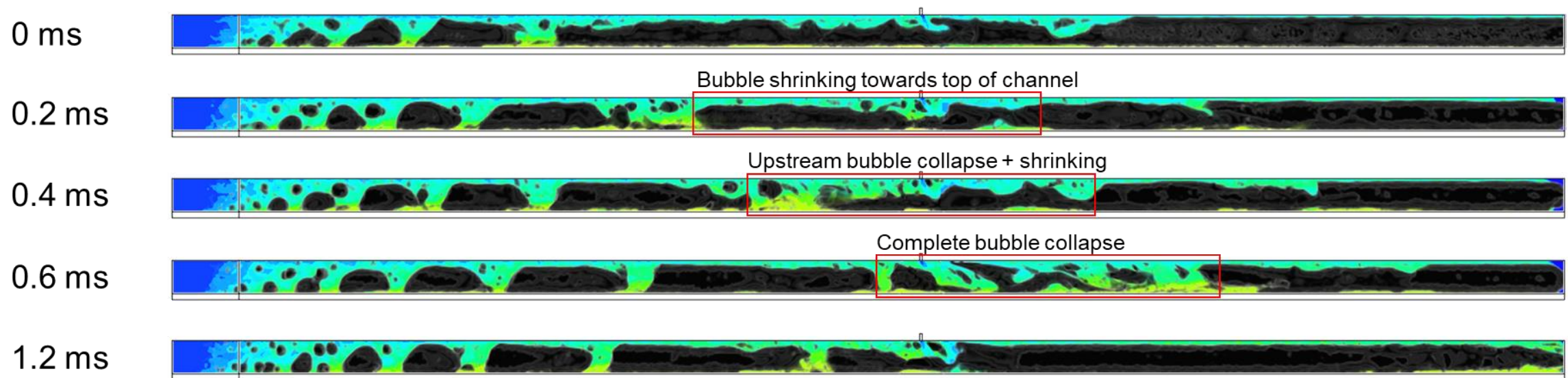
- Perform flow boiling experiments and simulations with dielectric fluids with metal foam
- Demonstrate vapor chamber performance for SiC MOSFET to achieve 1 kW/cm^2 heat flux removal with $200 \text{ }^\circ\text{C}$ operating temperature (in progress).
- Improve the performance of vapor chamber by optimizing different parameters
- Perform mechanical characterization of bond; compare AlN-AlSiC assembly to conventional DBC stack without cooling enhancement features
- Study formation and growth of intermetallic compounds within bond using X-ray diffraction and X-ray spectroscopy

➤ Electric motor thermal management

- Create a full computational fluid dynamics/heat transfer model of the stator + water-jacket + end-winding channels
- Develop the lumped parameter thermal network model for the complete Nissan Leaf motor to compute the torque versus speed characteristics with the proposed end-winding channel
- Optimize the design of the channel to reach the highest HTC for the lowest pumping power

Technical Back-Up Slides

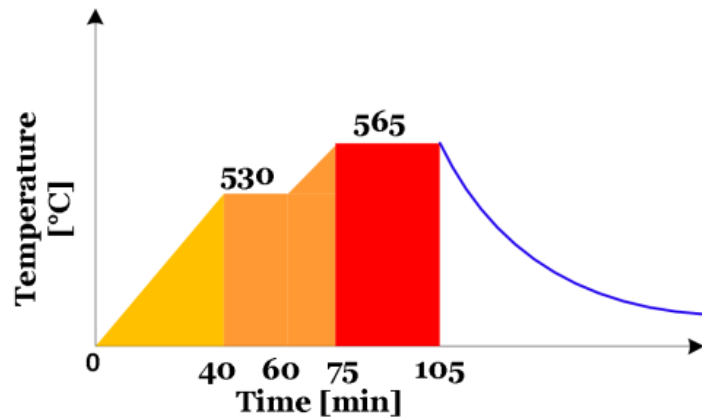
- Bubble visualization
 - Case 3: Bubbles begin to be confined and contact the outer sides of the channel, leading to cross-sectional views that are no longer axisymmetric
 - Case 4: Bubble begins shrinking from the inlet direction and decreasing in size. Eventually collapses and moves downstream until it is out of the channel. This time-varying mechanism causes a lower pressure drop by condensing some of the vapor.



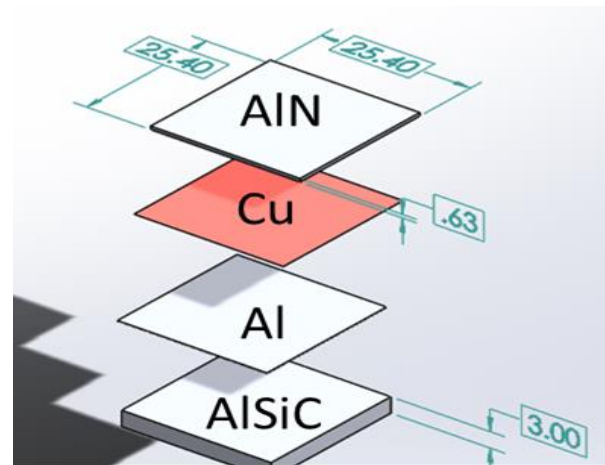
Bubble collapse and convection from auxiliary jetting, shown with vapor volume renders (in black) and temperature color contours

LOW THERMAL REISTANCE BONDED THERMAL INTERFACES: ACCOMPLISHMENTS

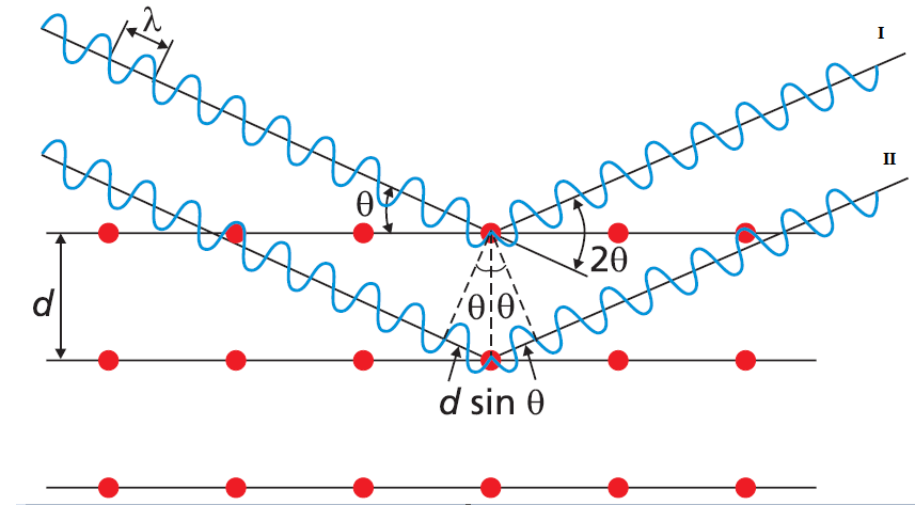
- **OBJECTIVE:** Determine Cu-Al intermetallic compounds formed during transient liquid phase bonding and effect on material properties
- Fabricated samples by bonding AlN, Cu and Al substrates to AlSiC heat sink using Cu-Al transient liquid phase bonding
- Conducted X-ray Diffraction tests along cross-sectioned surfaces of three different assemblies
- Results verified using SEM and EDS analyses



Temperature Profile



Sample Bond Stack



Bragg's Law

SciMed

$$n \lambda = 2d \sin \theta$$

Bragg's Law

d = Lattice Spacing

λ = Wavelength

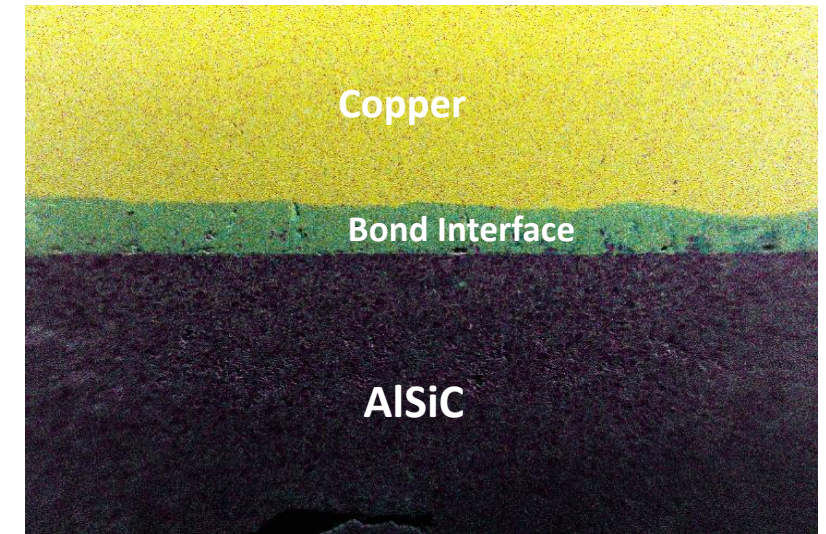
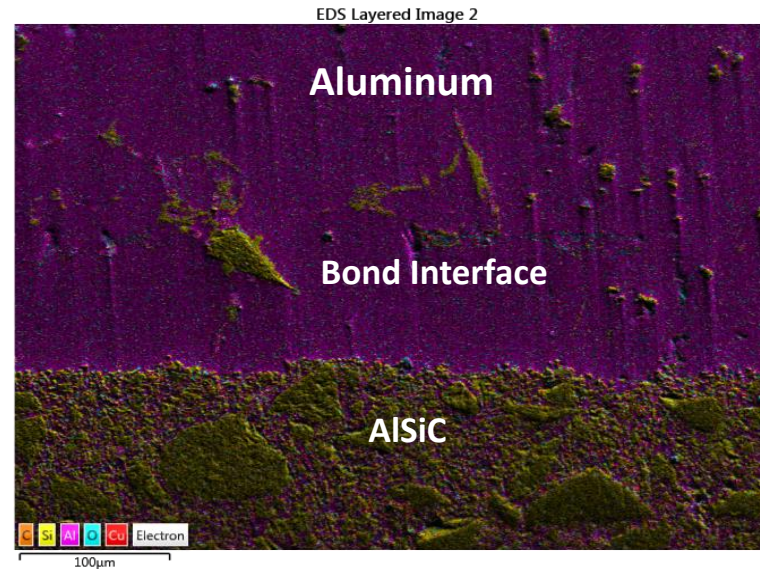
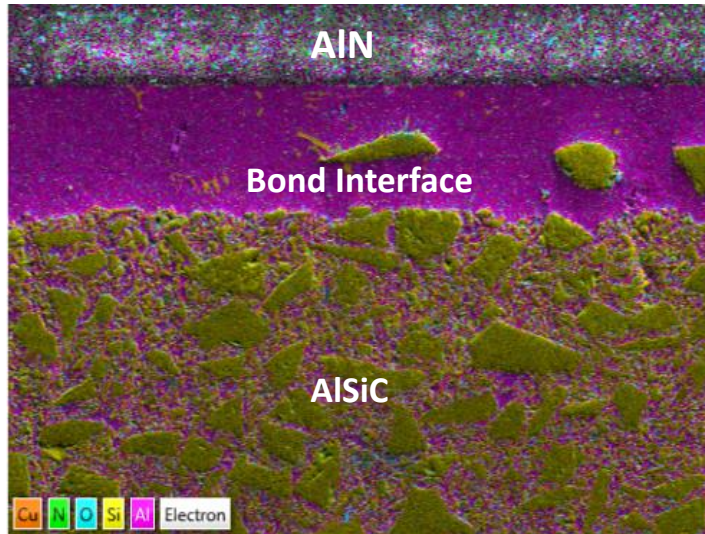
θ = Bragg angle

n = Integer order of interference

rows: atomic planes

*Condition for constructive interference

LOW THERMAL RESISTANCE BONDED THERMAL INTERFACES: OBSERVATIONS



- The intermetallic compound CuAl_2 (θ phase) was observed in all three samples via XRD and EDS analyses.
- However, in the case of 2mm Cu bonded to AlSiC, an additional phase Cu_9Al_4 was detected
- EDS line graph for AlN-AlSiC shows the volume fraction of Cu in the bond to be less than 2%, compared to Cu-AlSiC which had a higher concentration of Cu in the final composition of the bond
- This surplus Cu diffuses through the bond layer, reacting with Al in the AlSiC matrix to form a brittle intermetallic alloy as it solidifies

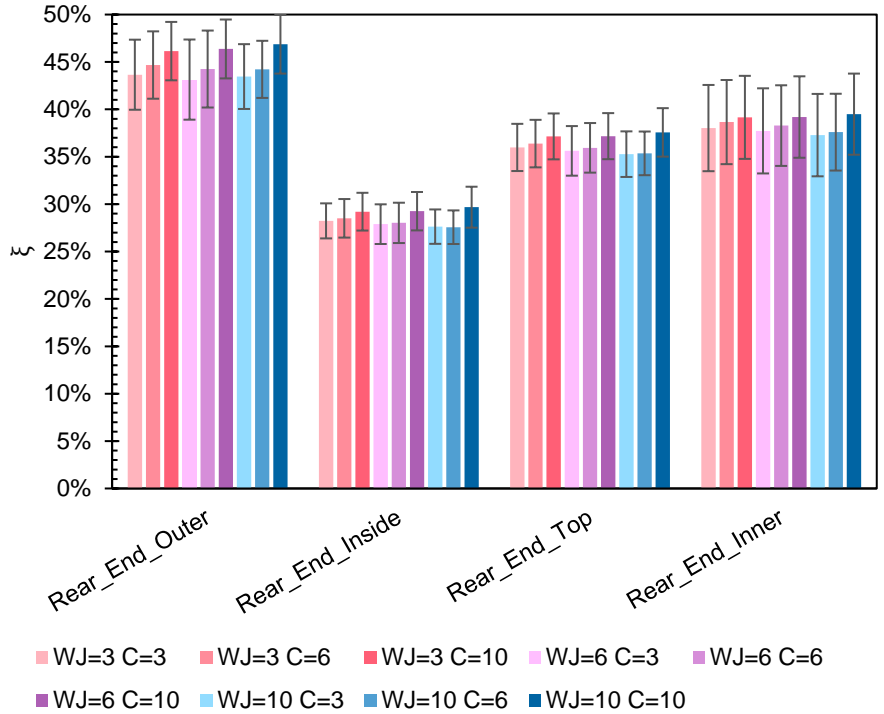
TECHNICAL ACCOMPLISHMENTS – ELECTRIC MOTOR THERMAL MANAGEMENT



PRELIMINARY RESULTS

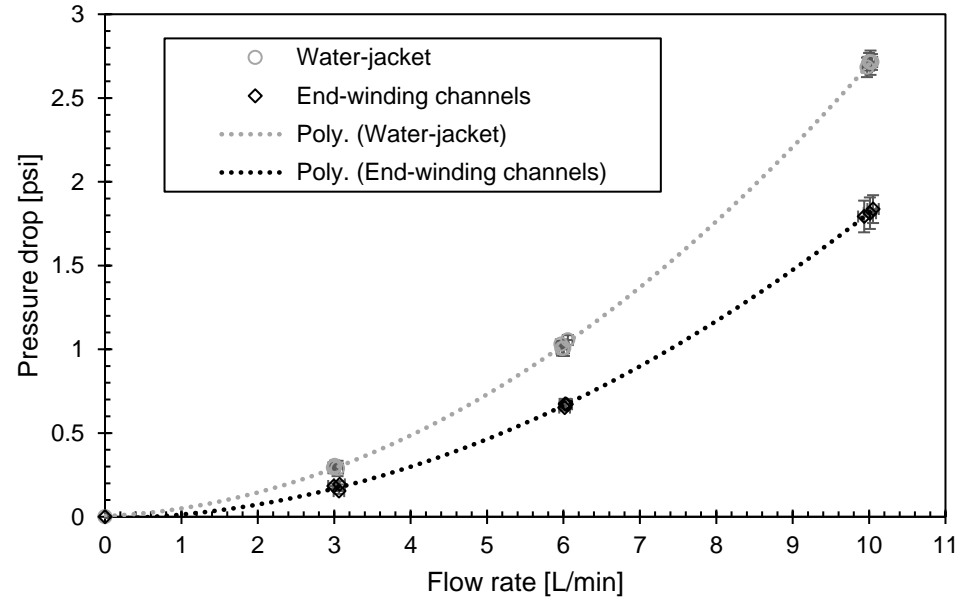
- The rate of temperature decrease ξ is derived between the solution with water-jacket only and the solution with both water-jacket and end-winding channel as follows (65 is the steady state temperature of end-windings without power input):

$$\xi = \frac{T_{water\ jacket\ only} - 65}{T_{water-jacket+end-wdg\ channel} - 65}$$



Rate of temperature decrease by using the end-winding channel at different flow rates in both the water-jacket and the end-winding channel

- Pressure-drop vs flow rate in the water-jacket and the end-winding channel has been derived. These values are suspected to be too high. We still need to understand what is influencing this high pressure drop.



TAKE-AWAYS

- On the outside surfaces (outer, inner and top), we have a minimum of 32% rate of temperature decrease!
- As the end-winding channel shows a good performance even at low flow rates and considering the low pressure drop at low flow rates for the channel, the additional pumping power for the channel is overcome by the cooling benefits of this solution.